Iran J Public Health, Vol. 53, No.10, Oct 2024, pp.2279-2289

Original Article

4-Methyl-N-(Piperidin-1-Ylmethylene) Benzenesulfonamide (PMSA) Promotes Ferroptosis of Tumor Cells by Targeting the *KEAP1-NRF2-GPX4* Axis

#Bingchun Sun [1], #Guangyu Zhao [1], Ligang Zhang [2], Jianji Hou [1], *Binhua Wu [1]

1. *The Marine Biomedical Research Institute, Department of Gynaecology and Obstetrics of Affiliated Hospital, Guangdong Medical University, Zhanjiang 524001, Guangdong, China*
2. *School of Medicine, Foshan University, Foshan 528225, Guangdong, China*

***Corresponding Author:** Email: wubinhua@gdmu.edu.cn
#These authors contributed equally to this work.

(Received 10 Jan 2024; accepted 19 Mar 2024)

Abstract

Background: We aimed to investigate the effect of 4-methyl-N-(piperidin-1-ylmethylene) benzenesulfonamide (PMSA) on tumor cell proliferation, migration, ferroptosis, and the potential molecular mechanism of ferroptosis in tumor cells.

Methods: PMSA was produced in the marine biomedical research institute of Guangdong Medical University (Zhanjiang, China) and used for tumor cells treatment. MTT and cell colony formation assays were used to measure the inhibition of tumor cell proliferation, the scratch assay was used to identified the suppression of tumor cell migration, the death of tumor cells was measured by Annexin-V-FITC/PI staining, the level of ferroptosis-relative lipid ROS in tumor cells was measured by flow cytometry and MDA detection kit, and the expression of ferroptosis-relative protein was measured by Western blot. The Discovery Studio system was used for molecular docking and the binding ability was measured by cellular thermal shift assay.

Results: The PMSA we produced inhibited tumor cell proliferation, colony formation, migration and triggered cell death, and Fer-1 could reverse these effects. The amount of ROS and MDA levels in tumor cells was also markedly raised by PMSA. PMSA treatment significantly reduced the expression of SLC7A11/XCT, *NRF2*, and *GPX4* in tumor cells. The phosphorylation level of *NRF2* was also decreased. Through molecular docking, it was discovered that PMSA could bind to *NRF2* and thereby block its activity.

Conclusion: The *KEAP1-NRF2-GPX4* axis was the target of PMSA's anti-tumor action, which results in ferroptosis of tumor cells. This demonstrated that the compound has the potential to be used as a candidate for anti-tumor drugs.

Keywords: Ferroptosis; Benzenesulfonamide; NF-E2-related factor-2; Glutathione peroxidase 4

Introduction

Cancers are malignant tumors that start in epithelial tissues and are extremely dangerous to one's health. The available medical therapies have a number of undesirable side effects and harm healthy tissues and cells (1). The advancement of contemporary medical technology has accelerated

the quest for novel cancer therapy approaches. Another emerging potential and significant therapeutic strategy for the treatment of cancer is the induction of ferroptosis in tumor cells (2).

Ferroptosis, a programmed death reliant on iron ions and reactive oxygen species (ROS) (3), has been implicated in the inhibition of tumor growth, opening up new therapeutic possibilities for cancer (4). Numerous genes and associated signaling pathways have been found to play a part in the control of ferroptosis in tumor cells (5). Among them, *nuclear factor erythroid 2-related factor 2* (*NRF2*) is an essential regulator of ferroptosis, which binds to the DNA sequence of antioxidant response elements (ARE) and triggers transcription of target genes. It is also involved in regulating cellular oxidative stress response, detoxification and drug resistance (6). *NRF2* can reduce tumor susceptibility and enhance tumor cell proliferation and protection against chemotherapy (7). *Kelch-like erythroid cell-derived protein with CNC homology-associated protein 1* (*KEAP1*) is a key regulatory factor controlling the transcriptional activity of *NRF2* (8). *Glutathione peroxidase 4* (*GPX4*) is a key downstream gene of *NRF2*, and mediates the catabolic breakdown of harmful lipid peroxides during lipid peroxidation (9). They together form the *KEAP1-NRF2-GPX4* gene axis, which not only regulates the proliferation and drug resistance of tumor cells, but also participates in ferroptosis (10). Therefore, this pathway is a convincing therapeutic target for tumor therapy based on (11).

Recent studies have so far demonstrated the anticancer potential of small compounds, nanomaterials, exosomes, and gene technologies based on the stimulation of ferroptosis in tumor cells (12). Amidines have a crucial role as both an essential medicinal moiety and as the structural backbone of small molecule medicines in pharmaceutical design and synthetic chemistry (13). There are not many studies on the use of sulfonamide derivatives in treating cancer, thus further research is needed to understand their precise molecular pathways. In order to examine its probable molecular mechanism of tumor proliferation and induction of ferroptosis in tumor cells, 4-methyl-N-(piperidin-1-ylmethylene) benzenesulfonamide (PMSA) was produced in the laboratory for the current investigation (14).

We aimed to investigate the effect of 4-methyl-N-(piperidin-1-ylmethylene) benzenesulfonamide (PMSA) on tumor cell proliferation, migration, ferroptosis, and the potential molecular mechanism of ferroptosis in tumor cells.

Materials and Methods

PMSA preparation and purity, structure verification

The sulfonamide derivative PMSA was produced in the marine biomedical research institute of Guangdong Medical University (Zhanjiang, China).

The synthesis method of PMSA was derived from Ghorab et al. (15) and shown in Fig. 1. PMSA was kept at a concentration of 25.90 mmol/L in dimethyl sulfoxide (DMSO). At room temperature, Piperidine (0.1 mmol) and p-Toluenesulfonyl azide (1.8 equiv) was mixed, then 3-Butyn-2-one was added carefully. The reaction mixture was stirred at room temperature for 2 minute to acquire PMSA. Silicagel 60 (230–400 mesh, Merck, Germany), and thin-layer chromatography (TLC) plates (Kieselgel 60F254, 0.25 mm, Merck, Germany) were used for column chromatography and analytical TLC, respectively. The purity of PMSA was detected by HPLC system using waters Alliance e2695 Separation Module with a photo-diode array detector (Waters 2998) and a reverse phase column (Waters Sunfire C18), mobile phase (methanol/H_2O). Structure verification was recorded on a Bruker Avance 400 MHz (Bruker, Fallanden, Switzerland).

Cell culture

The ovarian cancer cells SKOV3 and the prostate cancer cells 22RV1 were stored in our laboratory. They were cultured in DMEM medium (#8120365, Thermo Fisher Scientific, Shanghai, China) supplemented with 10% fetal bovine serum (#2279604CP, Thermo Fisher Scientific, Shanghai, China) and 1% penicillin-streptomycin (#P1400, Solarbio, Beijing, China). All cells were

routinely incubated at 37 ℃ in a humidified atmosphere of 5% CO_2.

Cell viability

Tumor cells were seeded into 96-well plates at the density of 5000 cells/well. After the adherent cell growth, cells were separately or jointly treated with PMSA and Fer-1 for 24 h. Cell viability was assessed using a MTT assay (#ST316, Beyotime, Shanghai, China), 10 μL thiazolyl blue tetrazolium bromide (MTT, 5 mg/mL) was added and incubated for additional 4 h. The supernatant was discarded and the precipitate was dissolved with DMSO. Absorbance of 570 nm was measured using a microplate reader.

Cell colony formation

Tumor cells were seeded into 6-well plates at the density of 1×10^6 cells/well and cultured until adherent. After 24 h, PMSA at different concentration were added and incubated for 10 d. Then, the cells were fixed with 4% polyoxymethylene at room temperature for 15 min. After washing with PBS for 3 times, cells were stained with crystal violet to observe the formation of colonies. Finally, the excess crystal violet was washed away and the number of colonies were counted under the microscope.

Cell scratch

Tumor cells were seeded into 6-well plates at the density of 5×10^5 cells/well. After 24 h, a single scratch was scratched in the monolayer cells in a straight line by a steriled 10 μL pipette tip. Then cells were incubated with DMEM alone or containing 10 μM PMSA. The photographs of the cell layer were taken at 0 and 24 h under an inverted microscope (Olympus, Tokyo, Japan). The width of the scratch was analyzed by ImageJ software and the migration rates were calculated.

Apoptosis assay

Tumor cells were seeded into 6-well plates at a density of 5×10^5 cells/well. After the adherent cell growth, cells were separately or jointly treated with PMSA and Fer-1. After incubation of 24 h, cells were collected with trypsin, washed twice with PBS and centrifuged at 1,500 rpm for 5 min. Subsequently, cells were subjected to apoptosis assay with Annexin V-FITC/PI Apoptosis Detection Kit (#C1062L, Beyotime, Shanghai, China) according to the instructions of manufacturer. Then, cells were analyzed using a BD Biosciences Fluorescence activated Cell Sorting (FACS, BD Pharmingen, NJ, USA) Calibur system with Cell Quest Pro software.

Measurement of reactive oxygen species (ROS)

Tumor cells were seeded into 6-well plates at a density of 1×10^5 cells/well overnight and then separately or jointly treated with PMSA or Fer-1 for 24 h. Cells then were treated with DCFH-DA (#S0033S, Beyotime, Shanghai, China) at 37 ℃ for 30 min. The ROS levels of collected cells were measured by FACS, indicated by fluorescence intensity.

Measurement of malondialdehyde (MDA)

Tumor cells were inoculated into 6-well plates at a density of 1×10^6 cells/well overnight and then incubated with PMSA or Fer-1 for 24 h. The cells were treated with cell lysate, and the protein concentration was determined with BCA protein concentration determination kit (#P0011, Beyotime, Shanghai, China). Lipid Peroxidation MDA Assay Kit (#S0131S, Beyotime, Shanghai, China) was used to measure the intracellular MDA level according to the kit instructions.

Western blot

Tumor cells were washed with PBS and lysed with RIPA buffer (#P0013E, Beyotime, Shanghai, China) containing protease and phosphatase inhibitors. Protein concentration was determined using BCA Protein Assay Kit. Protein was separated by polyacrylamide gel electrophoresis (PAGE) and transferred onto PVDF membrane. After blocking with 5% skim milk for 1 h at room temperature, the membrane was incubated with the appropriate primary antibodies at 4 ℃ overnight. Then, the membrane was washed with TBST for 3 times and incubated with secondary

antibody at room temperature for 1 h. Finally, protein blots were visualized using ECL substrate reagents. Primary antibodies (Sab, Jiangsu, China) used in western blot were as follows: *GPX4* (#32506), P62(#13222), ACSL4 (#36176), *KEAP1* (#32450), SLC7A11/XCT (#43437), *NRF2* (#41255), p-*NRF2* (#13360), HMOX1 (#32266) and GAPDH (#40493).

Molecular docking

Molecular docking study was demonstrated to investigate the interaction between PMSA and *NRF2*. The crystal structure of *NRF2* (PDB ID: 7k2k) was obtained from PDB database. The protein and ligand molecules were prepared by DS 3.5 software respectively before docking. Molecular docking of PMSA into the *NRF2* protein binding sites was performed by LibDock protocol. The LibDockScore was calculated after conducting the molecular docking.

Cellular thermal shift assay

SKOV3 cells were seeded into 6-well plates at a density of 1×10^6 cells/well overnight and treated with 10 μM PMSA for 24 h. The cells were collected, washed, resuspended in PBS with protease inhibitors and incubated with temperature gradient from 40-58 ℃ (100 μL/tube, 2 ℃ intervals) for 3 min in thermal cycler. The samples were incubated at room temperature for 3 min and transferred to liquid nitrogen for 3 min. The thermal shift procedures were conducted for 3 cycles and the cell lysates were subject to western blot assay to measure *NRF2* level. The binding stability between PMSA and *NRF2* was analyzed with the temperature melt curve.

Statistical analysis

All statistical analyses were conducted with GraphPad Prism 9.0 software. Values were shown as means ± SD and all experiments were repeated at least three times. Data were analyzed by one- or two-way ANOVA. The statistical significance of difference between groups was expressed by asterisks ($^{*}P < 0.05$, $^{**}P < 0.01$).

Results

Preparation and purity, structure verification of PMSA

The synthesis method and chemical structure of sulfonamide derivative PMSA was shown in Fig. 1A and B, chemical formula: $C_{13}H_{18}N_2O_2S$, molecular weight: 266.36. The synthesis yield, purity and product characteristics of PMSA were 82%, 99% and yellow solid (Fig. 1B and C). Structure of PMSA was verified via NMR spectra: ^{1}H NMR (400 MHz, $CDCl_3$) δ 8.10 (s, ^{1}H), 7.75 (d, J = 8.1 Hz, ^{1}H), 7.24 (d, J = 8.0 Hz, ^{1}H), 3.56 (d, J = 5.5 Hz, ^{1}H), 3.38 (d, J = 4.2 Hz, ^{1}H), 2.38 (s, ^{1}H), 1.80-1.58 (m, ^{1}H); ^{13}C NMR (100 MHz, $CDCl_3$) δ 157.3, 142.3, 139.7, 129.3 (2C), 126.5 (2C), 51.9, 44.7, 26.4, 24.9, 24.0, 21.5 (Fig. 1D).

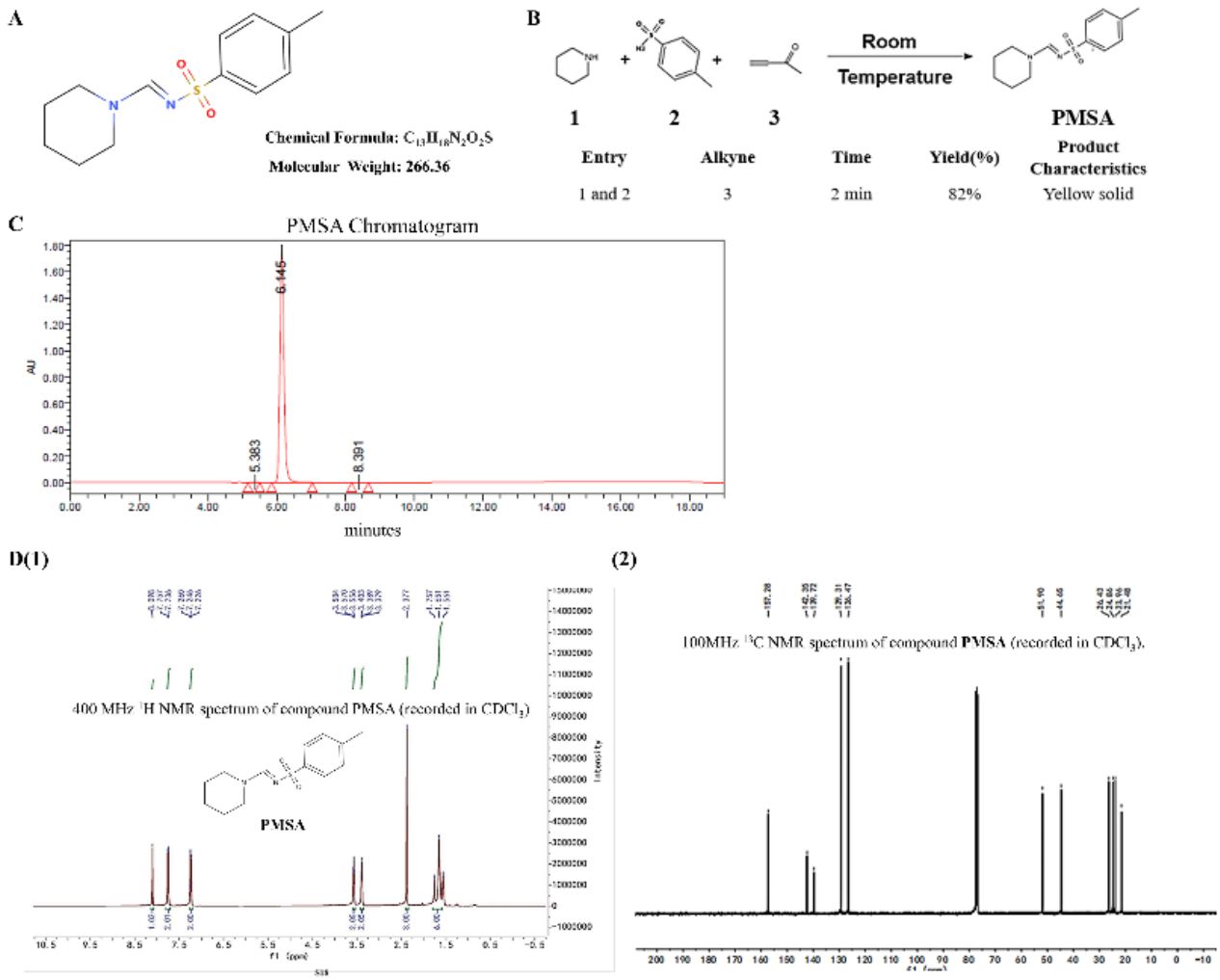

Fig. 1: Preparation and purity, structure verification of PMSA. (A) Chemical structural formula of PMSA. (B) Synthesis method of PMSA. (C) Purity verification of PMSA by HPLC system. (D) Structure verification of PMSA by NMR system

PMSA inhibited tumor cell proliferation and migration

To investigate the effect of PMSA on tumor cell viability, we employed a graded concentration of PMSA solution to treat tumor cells. PMSA could decrease the viability of tumor cells in a dose-dependent manner compared to the control group. Furthermore, the IC_{50} of PMSA in SKOV3 and 22RV1 cells was 3.451 μM and 1.182 μM, respectively (Fig. 2A).

Meanwhile, SKOV3 and 22RV1 cells were subject to cell colony formation experiments, respectively. Compared with the control group, the number of colony formation decreased in a dose-dependent manner with increasing concentration, and the difference was statistically significant. Comparing the two tumor cell lines, the effect of PMSA on SKOV3 cells was stronger, and it could be seen that PMSA produced a lower concentration of inhibition on SKOV3 cells and had a more pronounced effect on inhibiting proliferation (Fig. 2B, $^{**}P$ <0.01). Furthermore, cell scratch assay was used to confirm the repressed effect of PMSA on tumor cell migration (Fig. 2C, $^{**}P$ <0.01).

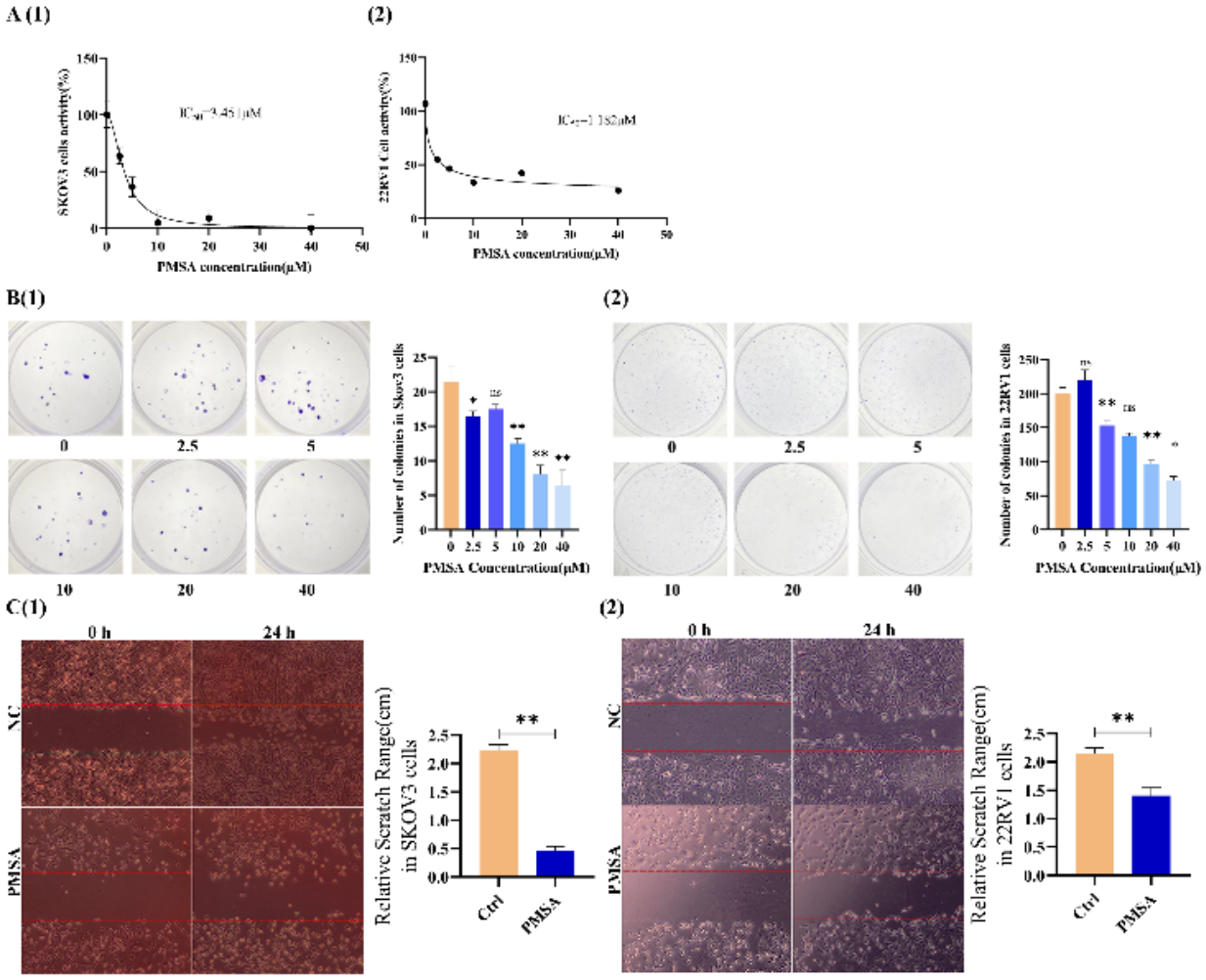

Fig. 2: PMSA inhibited tumor cell proliferation and migration. SKOV3 and 22RV1 cells were treated with 0-40 μM PMSA for 48 h, respectively. (A) MTT assay and IC_{50} of PMSA on tumor cells. (B) Cell colony formation assay of PMSA on tumor cells. (1) SKOV3 cells, (2) 22RV1 cells. (C) Cell scratch assay of PMSA on tumor cells. (1) SKOV3 cells, (2) 22RV1 cells. The error bars represented standard deviation from three replicates. $^{*}P < 0.05$ or $^{**}P < 0.01$ relative to the control or the differently treated groups, ns: no statistical difference

PMSA triggered ferroptosis in tumor cells

Ferrostatin-1 (Fer-1), a ferroptosis inhibitor, was used in the subsequent experiments. The results showed that compared with the control group, PMSA significantly inhibited the proliferation activity, aggravated the apoptosis effects in tumor cells, and increased the ROS and MDA levels, while fer-1 could rescue the cell death induced by PMSA above (Fig. 3A-D, $P < 0.05$, $P < 0.01$). PMSA could induce the tumor cell death via mediating ferroptosis effects.

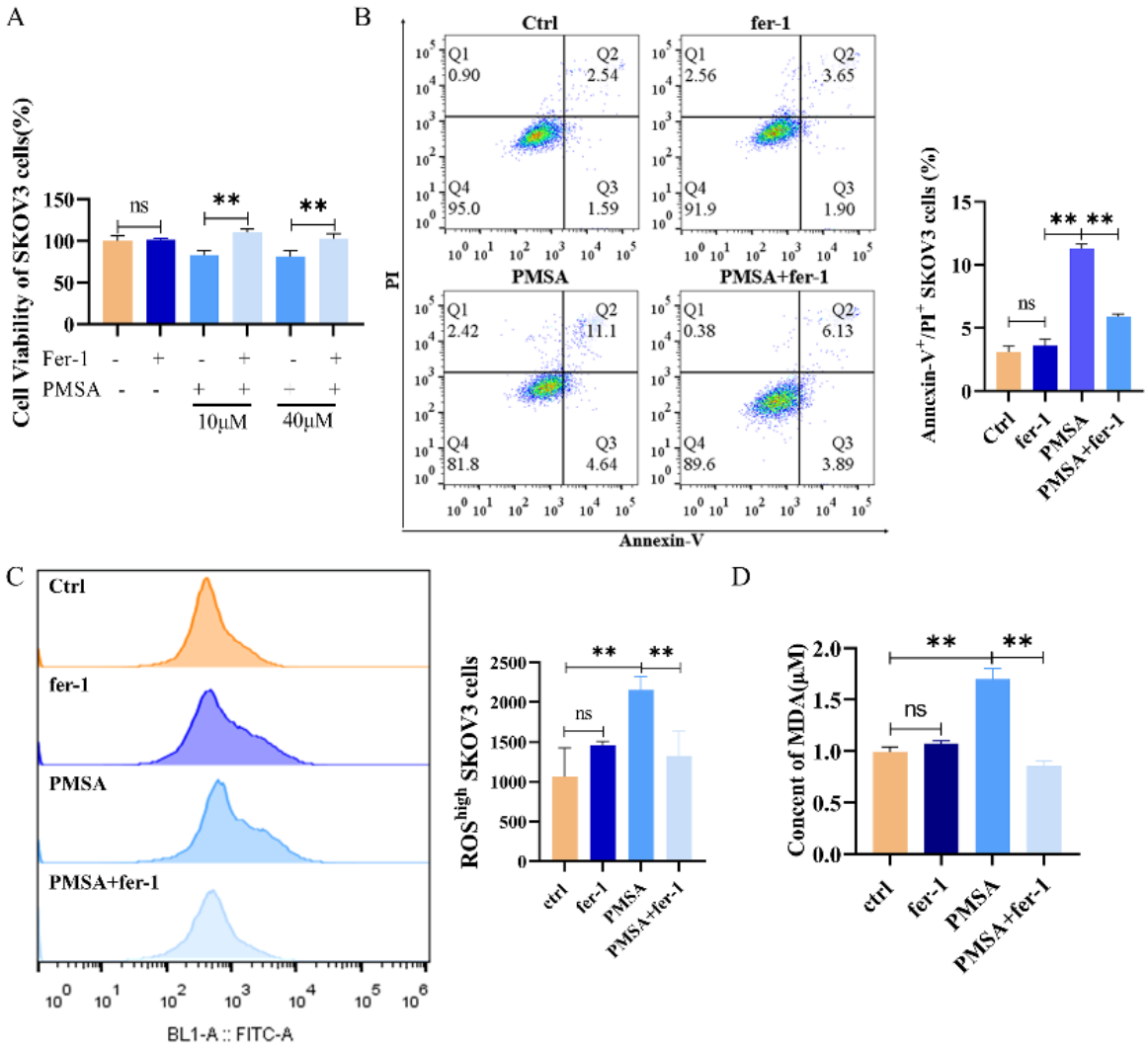

Fig. 3: PMSA induced tumor cell ferroptosis. (A) MTT assay of Fer-1 and different concentration of PMSA on SKOV3 cells. (B) Apoptosis assay of PMSA on SKOV3 cells. They were divided into 4 groups: blank control group, PMSA, Fer-1, PMSA and Fer-1. (C-D) Measurement of ROS levels (C) or MDA levels (D) in SKOV3 cells. They were divided into 4 groups: blank control group, PMSA, Fer-1, PMSA and Fer-1. The error bars represented standard deviation from three replicates. $^{**}P < 0.01$ relative to the control or the differently treated groups, ns: no statistical difference

PMSA regulated tumor ferroptosis through the KEAP1-NRF2-GPX4 axis

PMSA decreased *GPX4* protein expression in SKOV3 cells. In contrast, Fer-1 could rebound *GPX4* protein expression in a dose-dependent manner, which indicated that Fer-1 antagonized PMSA-induced ferroptosis (Fig. 4A, $^{**}P < 0.01$). Moreover, we revealed that PMSA also repressed the expression of ferroptosis-relative genes such as Solute Carrier family 7 member 11 (SLC7A11/XCT), *NRF2*, and p-*NRF2* in a dose-dependent manner in SKOV3 and 22RV1 cells (Fig. 4B and C, $^{*}P < 0.05$, $^{**}P < 0.01$). PMSA could regulated tumor ferroptosis through the *KEAP1-NRF2-GPX4* axis. Interestingly, the expression level of *KEAP1* increased.

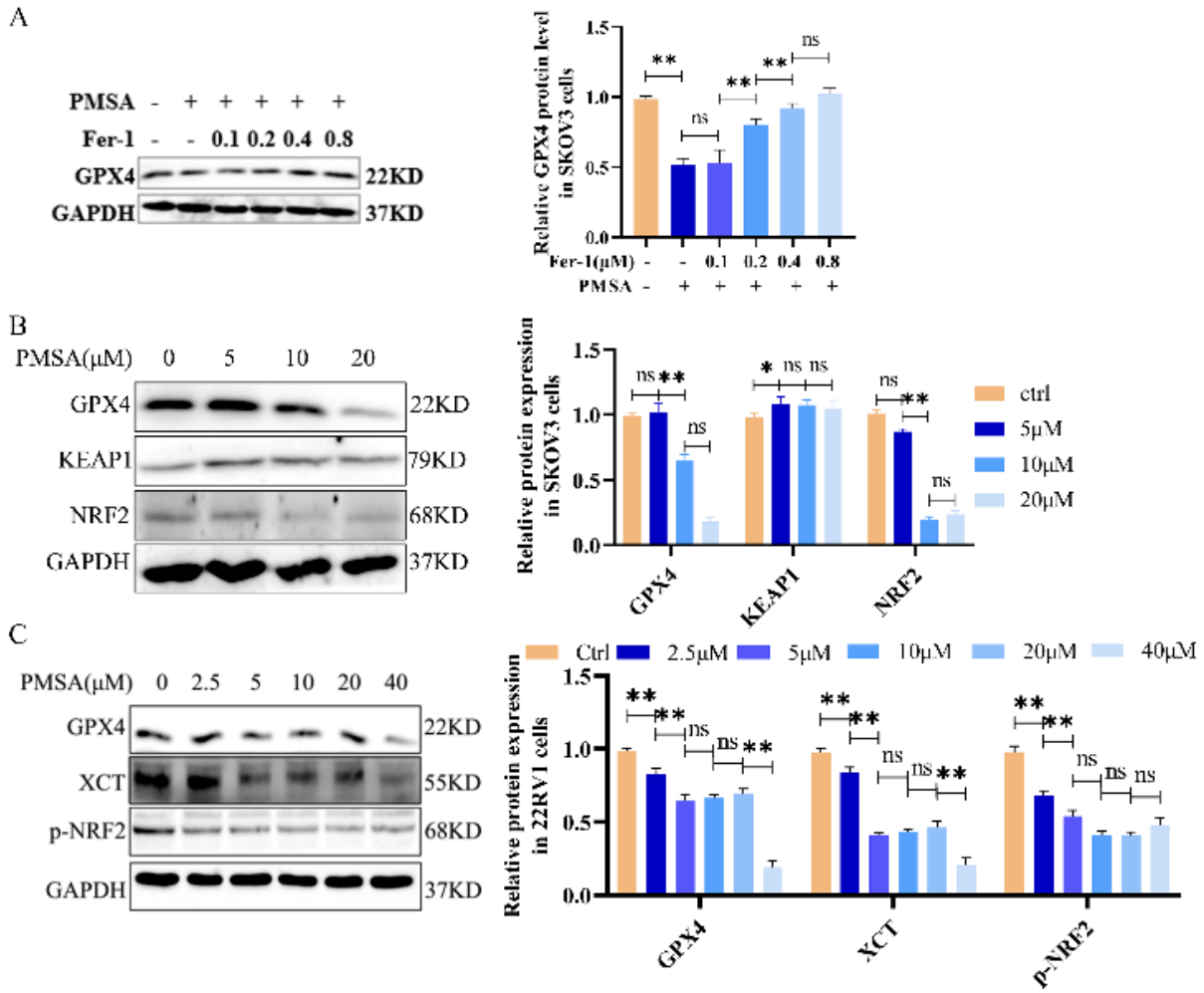

Fig. 4: Regulation of PMSA on ferroptosis-relative signaling pathways in tumor cells. (A) Western blot of *GPX4* levels in SKOV3 cells. (B) Western blot of *KEAP1*, *NRF2*, *GPX4* levels in SKOV3 cells. (C) Western blot of p-*NRF2*, XCT, *GPX4* levels in 22RV1 cells. The error bars represented standard deviation from three replicates. $^{*}P < 0.05$ or $^{**}P < 0.01$ relative to the control or the differently treated groups, ns: no statistical difference

PMSA triggered tumor ferroptosis by targeting NRF2 directly

Molecular docking confirmed the *NRF2* gene as a target of PMSA. As shown in Fig. 5A and B, PMSA could dock with *NRF2* protein with a LibDockScore of 95 and form a hydrogen bond at a distance of 2.78 Å at VAL418. Thermal stability studies were conducted to confirm the binding between PMSA and *NRF2* protein. The *NRF2* protein in the control group was rapidly degraded with increasing temperature, however, the experimental group did not exhibit substantial degradation of *NRF2* protein due to the addition of PMSA (Fig. 5C). Thus, PMSA might bind to *NRF2* protein and decreased its level in tumor cells, which mediated the ferroptosis effects and caused tumor cell death.

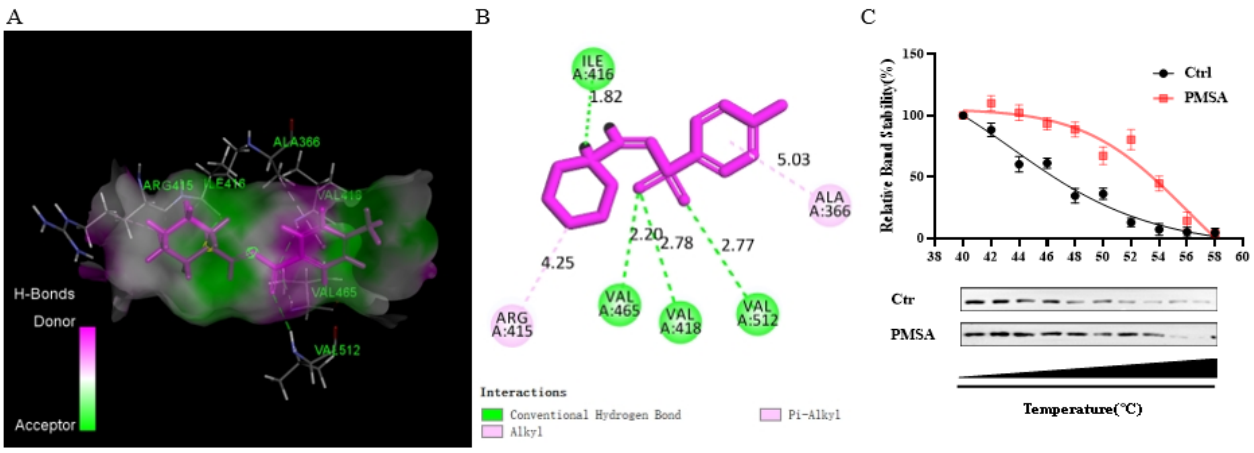

Fig. 5: Molecular docking of PMSA and *NRF2* protein ligands. (A-B) 3D views and binding sites of PMSA and *NRF2* protein ligands. (C). Thermal shift assay to analysis of band stability between PMSA and *NRF2* protein (40-58 ℃)

Discussion

Amidine is widely found in nature, and derivatives formed by its combination with sulfonamides may be responsible for the remarkable changes in biological activities and biological functions (e.g., anti-tumor and anti-fungal). Sulfamethoxyl, a derivative of amidine, is a molecule with multiple biological activities and can be utilized as an insecticide, but its anti-tumor properties and specific molecular mechanisms are still not clear (16). PMSA, a new sulfonamide derivative, was synthesized in our laboratory, and it has been previously demonstrated that it could inhibit the proliferation of tumor cells and then trigger cell death. According to bioinformatics analysis, PMSA might be involved in the regulation of ferroptosis-relative signaling pathways, and play an anti-tumor role by binding to *NRF2*. Therefore, in this study, we focused on the specific role of PMSA in tumor cells on ferroptosis pathway. Our results confirmed that PMSA could trigger ferroptosis in tumor cells by increasing lipid peroxidation (MDA) and ROS levels, but ferroptosis inhibitor Fer-1 prevented this by clearing ROS.

To identify the role of ferroptosis regulatory genes, we analyzed changes in the protein expression levels of these genes in tumor cells after treated with PMSA. The results showed that PMSA reduced the expression of *NRF2*, and *GPX4*, which indicated that it could induced tumor cells ferroptosis through the KEAP-*NRF2-GPX4* axis.

Furthermore, we investigated the interaction between PMSA and *NRF2* gene in depth. The results showed that PMSA could bind to *NRF2* protein and induced ferroptosis in tumor cells. At the same time, we also found that PMSA up-regulated *KEAP1* expression. This might be due to the competitive binding of PMSA to *NRF2*, which led to the dissociation of *KEAP1* protein from the *KEAP1*/*NRF2* complex in tumor cells (17). Compared with literature reading, it has been found that other sulfonamide derivatives also show anti-*NRF2* activity (18). However, PMSA demonstrated a stronger inhibitory effect with lower concentration.

It is noteworthy that PMSA controls the protein expression associated with the SLC7A11/XCT pathway (19). Another regulatory target of the *KEAP1*/*NRF2* pathway is SLC7A11/XCT pathway. SLC7A11 is a sodium-independent cystine-glutamate transporter. Extracellular cysteine is brought into cells by XCT, which converts it to cysteine to make glutathione (GSH). Reduced GSH synthesis may be caused by down-regulation of XCT, which triggers ROS-mediated ferroptosis (20). We found that PMSA reduced SLC7A11 protein levels in tumor cells, suggesting that it also

contributed to oxidative stress associated with the glutathione system.

Conclusion

PMSA could induce ferroptosis of tumor cells by targeting the *KEAP1-NRF2-GPX4* axis. This is an important discovery that this compound can be used as a potential anti-cancer drug. On basis of our investigations, we propose that PMSA deserves further studies as a small molecule targeted drug for discovering novel anti-cancer drug.

Journalism Ethical considerations

Ethical issues (Including plagiarism, informed consent, misconduct, data fabrication and/or falsification, double publication and/or submission, redundancy, etc.) have been completely observed by the authors.

Acknowledgements

This work was supported by the Fund of Southern Marine Science and Engineering Guangdong Laboratory (Zhanjiang) (ZJW-2019-007).

Conflict of Interest

The authors declare that there is no conflict of interest.

References

1. Vogelstein B, Papadopoulos N, Velculescu VE, Zhou S, Diaz LA Jr, Kinzler KW (2013). Cancer genome landscapes. *Science,* 339 (6127): 1546-1558.
2. Liu D, Li G, Jia A, Zhao Y, Cao C, Xing X (2018). Regulatory mechanism of ferroptosis, a new mode of cell death. *Trop J Pharm Res,* 17: 2309-2316.
3. Viswanathan VS, Ryan MJ, Dhruv HD, et al (2017). Dependency of a therapy-resistant state of cancer cells on a lipid peroxidase pathway. *Nature,* 547(7664): 453-457.
4. Mou Y, Wang J, Wu J, et al (2019). Ferroptosis, a new form of cell death: opportunities and challenges in cancer. *J Hematol Oncol,* 12(1): 34.
5. Chen X, Kang R, Kroemer G, Tang D (2021). Broadening horizons: the role of ferroptosis in cancer. *Nat Rev Clin Oncol,* 18: 280-296.
6. Cheng M, Wang P, Wu D (2022). Diosmetin alleviates periodontitis by inhibiting oxidative stress and pyroptosis via Nrf2/NF-κB/NLRP3 axis. *Trop J Pharm Res,* 21: 2303-2308.
7. Rojo de la Vega M, Chapman E, Zhang DD (2018). NRF2 and the Hallmarks of Cancer. *Cancer Cell,* 34(1): 21-43.
8. Wang W, Yang X, Chen Q, et al (2020). Sinomenine attenuates septic-associated lung injury through the Nrf2-Keap1 and autophagy. *J Pharm Pharmacol,* 72(2): 259-270.
9. Doll S, Proneth B, Tyurina YY, et al (2017). ACSL4 dictates ferroptosis sensitivity by shaping cellular lipid composition. *Nat Chem Biol,* 13(1): 91-98.
10. Shen K, Wang X, Wang Y, et al (2023). miR-125b-5p in adipose derived stem cells exosome alleviates pulmonary microvascular endothelial cells ferroptosis via Keap1/Nrf2/GPX4 in sepsis lung injury. *Redox Biol,* 62: 102655.
11. Dodson M, Castro-Portuguez R, Zhang DD (2019). NRF2 plays a critical role in mitigating lipid peroxidation and ferroptosis. *Redox Biol,* 23: 101107.
12. Liang C, Zhang X, Yang M, Dong X (2019). Recent Progress in Ferroptosis Inducers for Cancer Therapy. *Adv Mater,* 31(51): e1904197.
13. Bistrović A, Krstulović L, Harej A, et al (2018). Design, synthesis and biological evaluation of novel benzimidazole amidines as potent multi-target inhibitors for the treatment of non-small cell lung cancer. *Eur J Med Chem,* 143: 1616-1634.
14. Zhao Y, Zhou Z, Chen M, Yang W (2021). Copper-Catalyzed One-Pot Synthesis of N-Sulfonyl Amidines from Sulfonyl Hydrazine, Terminal Alkynes and Sulfonyl Azides. *Molecules,* 26(12): 3700.
15. Ghorab MM, Ragab FA, Heiba HI, Soliman AM (2016). Design and synthesis of some novel 4-Chloro-N-(4-(1-(2-(2-cyanoacetyl)hydrazono)ethyl)phenyl) benzenesulfonamide derivatives as anticancer and radiosensitizing agents. *Eur J Med Chem*, 117: 8-18.

16. Zhang S, Xiong P, Ma Y, et al (2022). Transformation of food waste to source of antimicrobial proteins by black soldier fly larvae for defense against marine Vibrio parahaemolyticus. *Sci Total Environ,* 826: 154163.
17. Nguyen LXT, Troadec E, Kalvala A, et al (2019). The Bcl-2 inhibitor venetoclax inhibits Nrf2 antioxidant pathway activation induced by hypomethylating agents in AML. *J Cell Physiol,* 234(8): 14040-14049.
18. Soliman AM, Karam HM, Mekkawy MH, et al (2020). Radiomodulatory effect of a non-electrophilic NQO1 inducer identified in a screen of new 6, 8-diiodoquinazolin-4(3H)-ones carrying a sulfonamide moiety. *Eur J Med Chem,* 200: 112467.
19. Duong HQ, Yi YW, Kang HJ, et al (2014). Inhibition of NRF2 by PIK-75 augments sensitivity of pancreatic cancer cells to gemcitabine. *Int J Oncol,* 44(3): 959-969.
20. Kirtonia A, Sethi G, Garg M (2020). The multifaceted role of reactive oxygen species in tumorigenesis. *Cell Mol Life Sci,* 77(22): 4459-4483.